Since January 2020 Elsevier has created a COVID-19 resource centre with free information in English and Mandarin on the novel coronavirus COVID-19. The COVID-19 resource centre is hosted on Elsevier Connect, the company's public news and information website.

Results in Chemistry 4 (2022) 100329

Contents lists available at ScienceDirect

Results in Chemistry

journal homepage: www.sciencedirect.com/journal/results-in-chemistry

Characterization, molecular modeling and pharmacology of some 2́-hydroxychalcone derivatives as SARS-CoV-2 inhibitor

Mohammad Nasir Uddin [a,*,1], Sayeda Samina Ahmed [a], Monir Uzzaman [a], Md. Nazmul Hassan Knock [a], Wahhida Shumi [b], Abul Fazal Md. Sanaullah [a], Md. Mosharef Hossain Bhuyain [a]

[a] Department of Chemistry, University of Chittagong, Chittagong 4331, Bangladesh
[b] Department of Microbiology, University of Chittagong, Chittagong 4331, Bangladesh

ARTICLE INFO

Keywords:
2-Hydroxychalcones
Antimicrobial and antioxidant assessment
SARS-CoV-2 main protease
Molecular docking
Dynamics
ADMET prediction

ABSTRACT

This work presented the microwave assisted synthesis of six new 2́-hydroxychalcones and their characterization based on FTIR, UV–Vis, ^{1}H NMR, and mass spectral analysis. Quantum chemical studies confirmed the structures of prepared chalcones. Antioxidant, *in vitro* antimicrobial and *in silico* antiviral studies have been performed to evaluate their biological performance. Results of molecular docking of prepared 2́-hydroxychalcones against SARS-CoV-2 (7BQY) main protease disclosed their inhibition which is comparable to standard, remdesivir and better than hydroxychloroquine (HCQ). ADMET prediction revealed them to be non-carcinogenic and relatively safe.

Introduction

World Health Organization announced corona virus 2019 (COVID-19), a viral respiratory disease in human, as pandemic disease [1]. Researchers are working vigorously to test a wide variety of potential COVID-19 treatments. The world was eagerly waiting for any hope in defying the COVID-19 pandemic when researchers focused the encouraging data from clinical trial of the antiviral drug such as hydroxychloroquine formerly used as the malaria drug or remdesivir previously trialed against the Ebola virus. While remdesivir reduces the mortality rate and the duration of the illness COVID-19, there is no magic remedy. On the other hand hydroxychloroquine is already considered as discarded drug against COVID 19 treatment. But no drug is still unanimously proved to be effective for the treatment of COVID-19. Besides in some cases side effects of the prescribed drugs are reported. As potential inhibiting properties of some chalcone derivatives are indicated [2,3], attention might be given on their probable applications in treatment of COVID-19.

Chalcones where two aromatic rings having diverse array of substituents are linked by an aliphatic three carbon chain are known as benzyl acetophenone or benzylideneacetophenone or *trans*-1, 3-diaryl-2-propen-1-ones. Two rings are interconnected by a highly electrophonic α, β-unsaturated carbonyl system containing the ketoethylenic group (–CO–CH=CH–). Chalcones having linear or nearly planar structure possess conjugated double bonds where π-electrons are delocalized on both rings [4,5]. This special structure of chalcones made them biologically active having high therapeutic value [6]. Therefore, chalcones exhibited tremendous potentiality as a pharmacological agent and their derivatives were proved to be suitable for the expansion of new medicinal agents possessing improved potency, lesser toxicity and good pharmacological actions. Chalcones are considered as important therapeutic potentials in the context of broad-spectrum biological activities including amoebicidal, antibacterial, anticancer, antihelmintic, antioxidative, antiprotozoal, antiulcer, cytotoxic, immunosuppressive and insecticidal properties [7]. Nowadays, chalcones are being used for the treatment of stomach cancer, cardiovascular diseases, viral disorders, pain, gastritis, and parasitic infections [7].

The potential anti-viral activities of chalcones have been well recognized via various targets including glyceraldehyde-3-phosphate dehydrogenase (GAPDH), topoisomerase-II, fumarate reductase, lactate dehydrogenase, several protein kinases, protein tyrosine phosphatase, human immunodeficiency virus (HIV-integrase (IN)/protease), lactate/isocitrate dehydrogenase, etc. [8].

Consequently, with the proven antiviral role of chalcones, they

* Corresponding author.
E-mail address: mnuchem@cu.ac.bd (M. Nasir Uddin).
[1] ORCID ID: 0000-0003-1235-2081

https://doi.org/10.1016/j.rechem.2022.100329
Received 24 November 2021; Accepted 15 March 2022
Available online 16 March 2022

became a new attractive subject of interest to the scientific community. Different types of chalcones are reported to act on important targets in diseases caused by viral infections [9,10]. The promising diverse antiviral bioactions made chalcone derivatives a favourable broad-spectrum candidate for targeting the most recent viral pandemic, COVID-19 [11,12]. Several scientific investigations focused the interesting biological activities of chalcone derivatives as potential pharmacological agents capable of targeting a variety of human viruses including; Middle East respiratory syndrome coronavirus MERS-CoV, severe acute respiratory syndrome related coronavirus (SARS-CoV) [13].

In this study, six 2́-hydroxychalcones belonging to two groups were synthesized by an eco-friendly microwave assisted method; one with different substituent in one benzene ring and other one with replacing benzene ring by a heterocyclic ring in one site of ketoethylenic group as to introduce a new group of chalcones. Anti-bacterial, antifungal and antioxidant activities were tested. Emphasizing the present demand molecular docking, nonbonding interaction, and ADMET calculation have been performed to investigate the potentiality of chalcones as antiviral drag against main protease of SARS-CoV-2 (7BQY).

Experimental

Chemicals and instrumentations

Solvents and reagents of analytical grade were purchased from Merck and used without any further purification. All reactions were carried out in a commercially available LG microwave oven (MB-3947C) having a maximum output of 800 W operating at 2450 MHz. The ^{1}H NMR spectra were taken by a Bruker Advance DPX 500 MHz spectrometer in $CDCl_3$ from "Wazed Miah Science Research Centre (WMSRC), Jahangirnagar University, Dhaka, Bangladesh using tetramethylsilane (TMS) as a standard. FTIR spectrophotometer (Model-8900, Shimadzu, Japan) was used to record spectra on KBr pellets. Samples were dissolved in $CHCl_3$ to take mass spectra using Agilent 6460 Triple Quad LC/MS. Autoclave Machine (ALP Co. Ltd. Japan), Laminar Airflow (BIOQUELL Medical Ltd.UK) and Incubator were adjusted at 35 ± 2 °C.

Synthesis of 1-(2′-hydroxyphenyl)-3-(substituted)furan-prop-2-en-1-one (1–3)

2′-hydroxychalcones **(1–3)** were synthesized from 2-hydroxyacetophenone and (substituted) furaldehyde under microwave condition. 10 mL of ethanolic KOH (10%) solution was added to 2′-hydroxyacetophenone (6 mmol) and furaldehyde (substituted) (6 mmol) placed previously in a porcelain dish and mixed well. The mixture was irradiated under 160 W microwave irradiation for 3 min 40 sec. The progression of the reaction was checked by TLC (n-hexane: ethyl acetate, 6:1). Ice cold water was acidified with dil. HCl and the reaction mixture was diluted with it and product was extracted with ether. The ether layer was washed with water, dried over anhydrous Na_2SO_4 and the solvent was evaporated when light yellow crystal of the product was obtained. The yellow crude solid was recrystallized from ethyl acetate and n-hexane to give as crystal.

The structural analyses of the compound **(1)** by spectroscopic methods are given below:

*1-(2′-hydroxyphenyl)-3-furan-prop-2-en-1-one **(1)***

Colour: yellow, **Yield:** 86.96%, **Melting Point:** 83–85 °C; **IR (KBr) ν_{max} (cm^{-1}):** 3501.09 (C-OH), 3013.90, 2970(C–H), 1641.49 (>C=O), 1583.63 (C=C), 1554.69, 1474.69 (C=C, Ph), 1215.21(C-O). **^{1}H NMR (400 MHz, $CDCl_3$):** δ_H (ppm): 6.57 (q, 1H, C_3-H), 6.80 (d,1H,J = 8 Hz C_2-H), 6.94 (d, 1H, J = 8 Hz, C_4-H), 7.05 (d, 1H, J = 8 Hz, $C_{3'}$-H), 7.54 (m, 2H,$C_{4'}$-H and $C_{5'}$-H), 7.56 (d, 1H, J = 15.2 Hz, C_α-H), 7.69 (d, 1H, J = 14.8 Hz, C_β-H), 7.96 (d, 1H, J = 8 Hz, $C_{6'}$-H), 12.90 (s, 1H, $C_{2'}$-OH). **Mass (*m/z*)** 213.56 (214), **Element (%):** C 72.34 (72.90), H 4.71 (4.67).

*1-(2′-hydroxy-phenyl)-3-(5-methyl-furan)-prop-2-en-1-one **(2)***

Colour: light yellow, **Yield:** 88.16%, **Melting Point:** 128 °C; **IR (KBr) ν_{max} (cm^{-1}):** 3520 (O–H), 1648 (C=O), 1612 (C=C of Ar), 1505 (CH=CH); **^{1}HNMR (400 MHz, $CDCl_3$):** 2.61 (3H, s, CH_3), 7.38 (1H, d, J = 17 Hz, –CO-CH=), 7.52 (1H, d, J = 17 Hz, =CH-Ar), 6.89 (1H, s, Ar-OH), 7.18–7.79 (6H, Ar-H); **Mass (*m/z*)** 227.96 (228.25), **Element (%):** C 73.74 (73.60), H 5.13 (5.26).

*1-(2′-hydroxy-phenyl)-3-(5-methoxy-furan))-prop-2-en-1-one **(3)***

Colour: yellow, **Yield:** 85.14%, **Melting Point:** 89 °C; **IR (KBr) ν_{max} (cm^{-1}):** 3460 (O–H), 1652 (C=O), 1585 (C=C of Ar), 1462 (CH=CH), 1127 (-O-CH_3),; **^{1}HNMR (400 MHz, $CDCl_3$):** 3.78 (3H,s, –OCH_3), 7.15 (1H, d, J = 17 Hz, –CO-CH=), 7.64 (1H, d, J = 17 Hz, =CH-Ar),

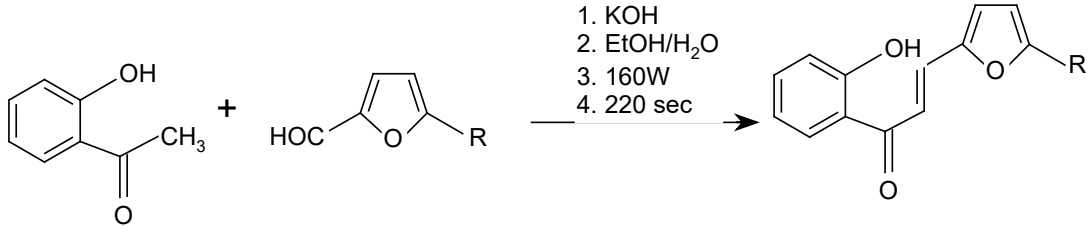

Compound 1. R= H; 2. R= CH_3; 3. R= OCH_3

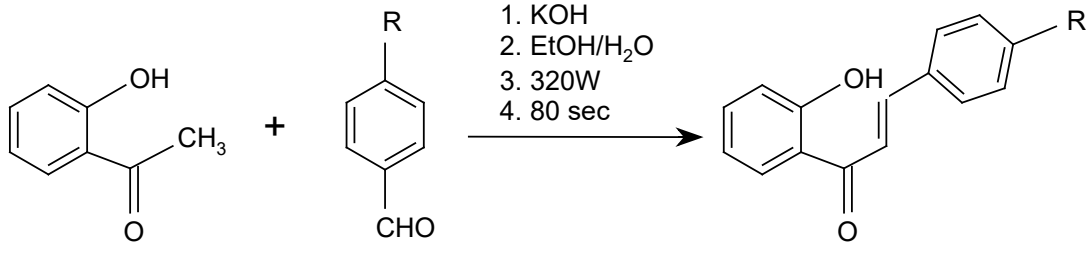

Compound 4. R= OH; 5. R=NO_2; 6. R= $N(CH_3)_2$

Fig. 1. Schematic presentation of synthesis of Chalcones.

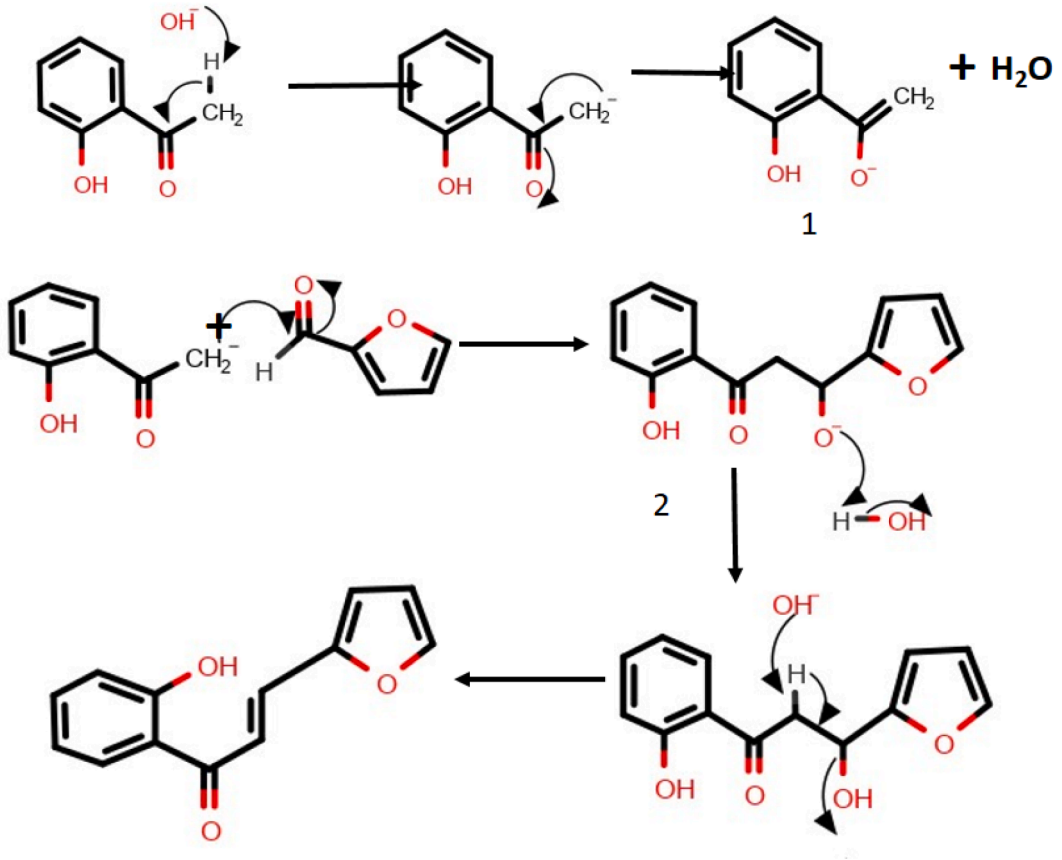

Scheme 1. Mechanistic presentation of *(2E)* 1-(2-hydroxyphenyl)-3-furan-prop-2-en-1-one synthesis.

7.12–7.58 (4H, Ar-H), **Mass (*m/z*)** 245.06 (244.25); **Element (%):** C 67.74 (68.78), H 5.13 (5.32).

Synthesis of 3-(4-hydroxyphenyl)-1-(substituted)phenyl-prop-2-en-1-one (4–6)

2′-hydroxychalcones **(4–6)** were synthesized from 2-hydroxyacetophenone and benzaldehyde (derivatives) under microwave condition. For the synthesis of 2′-hydroxychalcones **(4–6),** 10 mL of ethanolic KOH (10%) solution was added to the mixture of 2-hydroxyacetophenone (6 mmol) and benzaldehyde (derivatives) (6 mmol) placed in a porcelain dish and mixed well. Microwave irradiation under 320 W was irradiated on the mixture put in the microwave oven for 1 min 20 sec. The improvement of the reaction was observed by TLC (n-hexane: ethyl acetate, 6:1). Ice cold water was acidified with dil. HCl and the reaction mixture was diluted with it. The product was extracted with ether, washed with water, dried over anhydrous Na_2SO_4 and the solvent evaporated. The yellow crude solid was recrystallized from ethyl acetate and n-hexane.

The structural analyses of the compound (4–**6)** by spectroscopic methods are given below:

3-(4-hydroxyphenyl)-1-(2-hydroxyphenyl)-prop-2-en-1-one (4)

Colour: Greenish yellow, **Yield:** 88.16%, **Melting Point:** 129 °C; **IR (KBr) ν_{max} (cm^{-1}):** 3226 (–OH), 1692 (C=O), 1636 (C=C, aliphatic), 1562 (C=C, aromatic); **^{1}HNMR (400 MHz, $CDCl_3$):** 5.78 (Ar-OH), 7.6–8.36 (Ar-H), 3.8 (HC=CH); **Mass (*m/z*)** 240.96 (240.26); **Element (%):** C 74.74 (74.92), H 5.11 (4.99).

1-(2′-Hydroxyphenyl)-3-(4-nitro-phenyl)- prop-2-en-1-one (5)

Colour: Golden yellow, **Yield:** 88.16%, **Melting Point:** 128 °C; **IR (KBr) ν_{max} (cm^{-1}):** 3236 (–OH). 1670 (C=O), 1630 (C=C, aliphatic), 2835 (–NO_2), 1598 (C=C, aromatic); **^{1}HNMR (400 MHz, $CDCl_3$):** 5.80 (Ar-OH), 7.44–8.21 (Ar-H), 3.32 (HC=CH); **Mass (*m/z*)** 270.16 (269.26); **Element (%):** C 66.74 (66.85), H 4.11 (4.09), N 5.11 (5.20).

1-(2′-hydroxyphenyl)-3-(4-(N,N-dimethylaminophenyl)-prop-2-en-1-one (6)

Colour: yellow, **Yield:** 1.6942 g, (98.96%), **Melting Point:** 147–148 °C; **IR (KBr) ν_{max} (cm^{-1}):** 3495.16 (C-OH), 3015, 2976(C–H), 1661.75 (>C=O), 1575.9 (C=C), 1489.11 (C=C, Ph), 1339.62 (C-N), 1230.65 (C-O), 1035.82. **^{1}H NMR (400 MHz, $CDCl_3$):** δ_H (ppm): 3.08 (s, 6H, C_4-N(CH_3)$_2$), 6.74 (d, 2H,J = 8 Hz C_3-H and C_5-H), 6.96 (d, 1H, J = 8 Hz, $C_{3'}$-H), 7.02 (d, 1H,J = 8 Hz $C_{6'}$-H), 7.48 (m,1H $C_{5'}$) 7.61(d, 1H, J = 15.2 Hz, C_α-H), 7.7 (d, 2H, J = 8 Hz, C_2-H and C_6-H), 7.94 (d, 1H, J = 15.2 Hz, C_β-H), 7.96 (m, 1H, $C_{4'}$-H), 13.21 (s, 1H, $C_{2'}$-OH). **Mass (*m/z*)** 264.9 (267), **Element (%):** C 76.74 (76.31), H 6.11 (6.36), N 5.11 (5.24).

Fig. 1 shows the schematic presentation of *synthesis of 2′-hydroxychalcone.* Scheme 1 and 2 showed the mechanistic presentation of two representative *2′-hydroxychalcone* synthesis.

Computational study

Geometry optimization

Computational chemistry is becoming popular media to calculate the physicochemical and spectral properties [14]. Based on characterization result, structural drawing and optimization were carried out in Gaussian 16 software [15]. Density functional theory (DFT) based on Becke's (B)

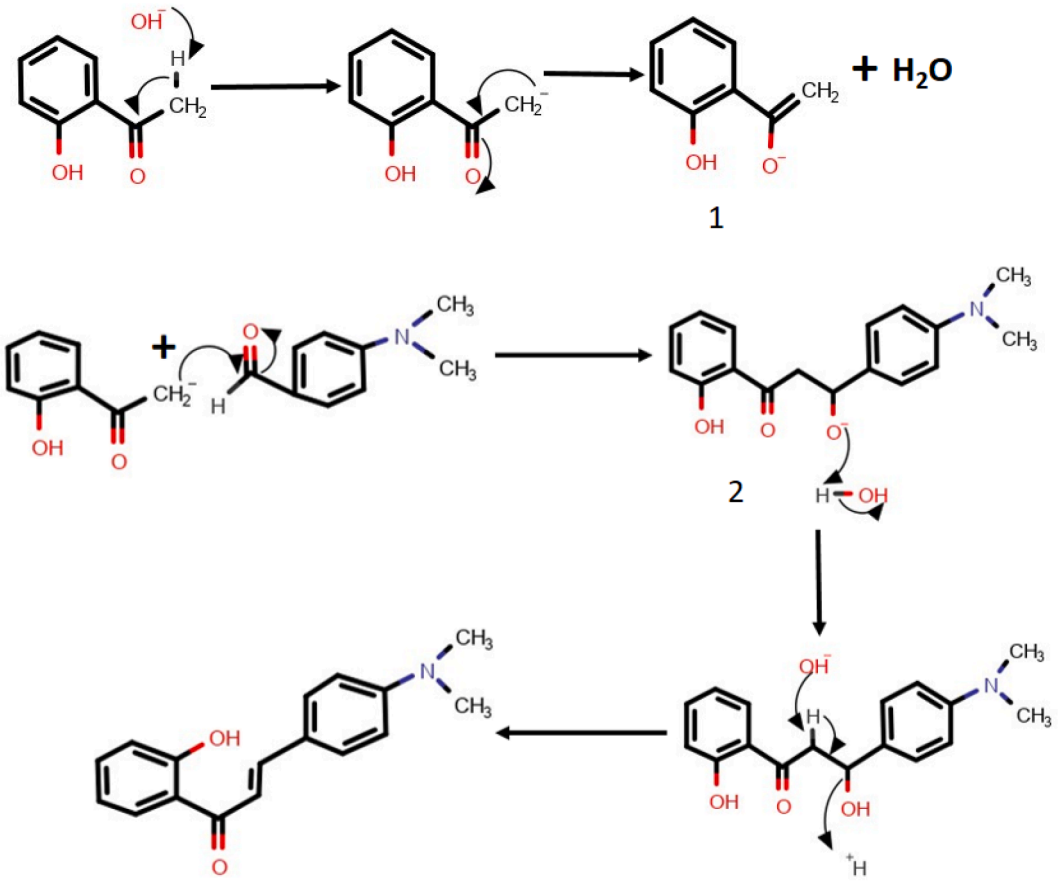

Scheme 2. Mechanistic presentation of (*2E*) 1-(2′-hydroxyphenyl)-3-(4-(N, N-dimethylamino phenyl)- prop-2-en-1-one synthesis.

[16] exchange functional combining Lee, Yang and Parr's (B3LYP) correlation functional methods [17] with 3–21 g basis set was employed to optimize and characterize the molecules which has amply been proven to give very good ground state geometries [18]. Frontier molecular orbital features HOMO (highest occupied molecular orbital), LUMO (lowest unoccupied molecular orbital) were calculated at the same level of theory. From the energies of frontier HOMOs and LUMOs as previously reported, hardness (η), softness (S), and chemical potential (μ) were calculated for each of the compounds [18] considering Parr and Pearson interpretation [19] of DFT and Koopmans theorem [20] on the correlation of ionization potential (*I*) and electron affinities (*E*) with HOMO and LUMO energies (ε). The following equations are used to calculate hardness (η), chemical potential (μ) and softness (S);

$$\eta = \frac{1}{2}[\varepsilon LUMO - \varepsilon HOMO];\ \mu = \frac{1}{2}[\varepsilon LUMO + \varepsilon HOMO];\ S = \frac{1}{\eta}$$

Protein preparation, docking and visualization

The 3D crystal structure of SARS-CoV-2 main protease was collected from RCSB protein data bank (PDB) database (PDB ID: 7BQY) [21]. The energy of the protein was minimized using Swiss-Pdb viewer software (version 4.1.0) because there are some issues regarding to improper bond order, side chains geometry and missing hydrogen (s) in the structure [22]. All hetero atoms and water molecules in crystal were eliminated using PyMol (version 1.3) software packages [23,24]. Discovery studio (Version 4.1) was utilized to calculate, and visualize the nonbonding interactions.

ADMET prediction

ADMET prediction implies chemical absorption, distribution, metabolism, excretion and toxicity (ADMET) those play an important role in drug discovery. A potential drug candidate should have sufficient efficiency against target and also have appropriate ADMET parameters. AdmetSAR online database has been utilized to predict pharmacokinetic properties of synthesized compounds [25].

Antimicrobial activities

Four human pathogenic bacteria e. g. *Escherichia coli, Bacillus subtilies, Salmonella paratyphi, Staphylococcus aureus* and two fungi e. g. *Aspergillus niger, Aspergillus flavus* collected from the Department of Microbiology, University of Chittagong, Bangladesh were selected to investigate antimicrobial activities of prepared chalcones. The liquid culture method [26] was followed for the detection of antibacterial activities measuring absorbance at 510 nm by spectrophotometer. Results of the antimicrobial activities were represented in graphs when results were compared to that of a standard, Ciprofloxacin (Sigma-Aldrich). 0.002 g and 0.008 g solid samples of tested compounds and antibiotic were dissolved in 1 mL ethanol prepare 0.1% and 0.8% solutions. Solid samples were dissolved completely in ethanol and also as it has no inhibitory effect on the cultures it was chosen as solvent.

Bacterial culture and sensitivity spectrum analysis

Standard Nutrient Broth media (NA) having the composition, Peptone (5 g), Beef Extract (3 g), NaCl (0.5 g) and Distilled water (1000 mL), was used throughout the study [27]. 24 h old culture was transferred to the test-tubes with the help of sterilized needles to prepare test tube slants of NA medium for the maintenance of cultures. Small amount of the microorganisms were transferred to the test tubes containing nutrient agar. Tubes were inoculated and incubated at 35 ± 2 °C for 24 h. The test tubes were capped with cotton placing 10 mL of prepared nutrient broth and sterilized at 121 °C for 20 min by autoclaving at 15-

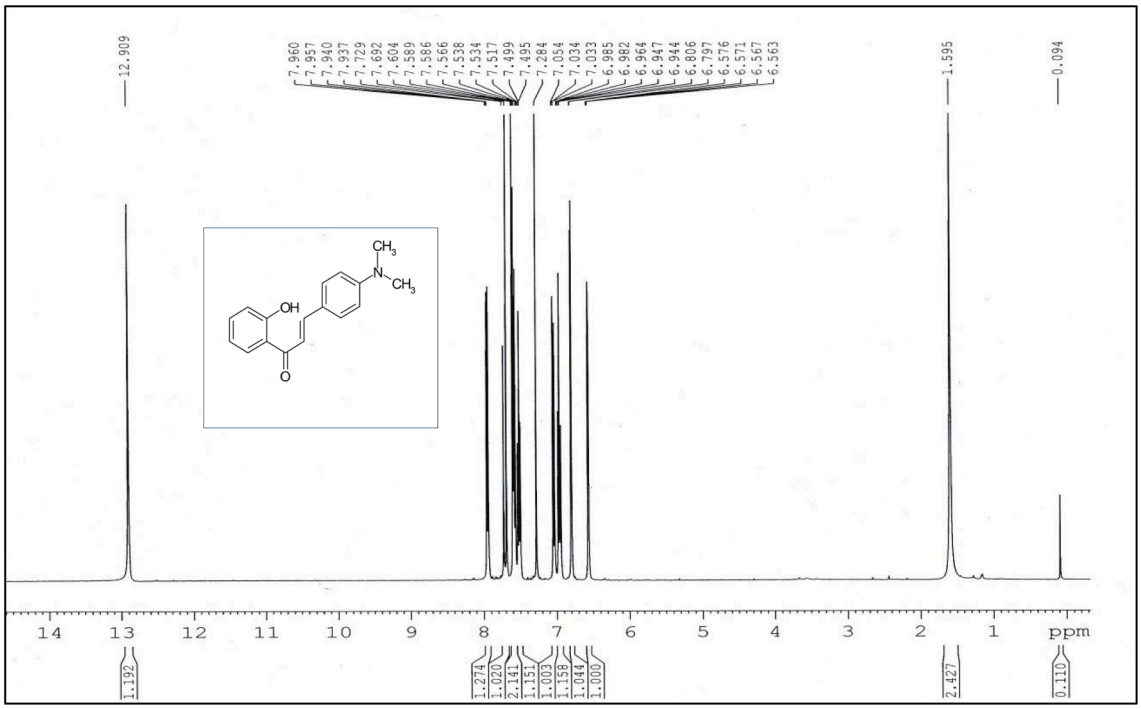

Fig. 2. ^{1}H NMR spectrum of the compound, 2'-hydroxy-4-(N, N-Dimethylamino)chalcone (6).

lbs. pressure/sq. inch. 100 μL test solutions were added to the sterilized nutrient broth and 100 μL incubated (at 37 °C) selected microorganisms were carefully inoculated to these test tubes. The absorbance of every incubated solution was recorded by UV-Spectrophotometer at 510 nm sequentially after 3, 6, 18 and 21 h.

Fungal cultures suspension and effects on fungal growth

For the growth and maintenance of fungal isolates, Potato Dextrose Agar (PDA) medium was used throughout the study [27]. The PDA was prepared by the composition of Potato (200 g), Dextrose (20 g), Agar (15 g) and Distilled Water (1000 mL). Potato Dextrose liquid culture medium was prepared without Agar which was used for the evaluation of fungal activity against test compounds.

After pouring on sterilized Glass Petri plates, 10 mL of the molten sterilized PDA medium was left for solidification. To the center of each PDA plate, small portion of each fungus mycelium was placed carefully with the help of sterilized needles. Equal amount of fungal mat were mixed with 50 mL of sterilized Potato Dextrose Liquid medium. Mixture was shaken well to mix thoroughly and suspension so prepared was used as stock culture for the test.

100 μL of test compounds (0.1% concentration) were added to 50 mL of sterilized potato dextrose liquid medium dispensed into 200 mL conical flasks. Each of the flasks was labeled and shaken well to mix thoroughly. After addition of 1 mL fungal suspension carefully, conical flasks were incubated at 27 ± 2 °C for 5 days. A control conical flask was prepared with ethanol instead of test compounds. The fungal biomass growth was observed and recorded after 4 days incubation. After filtration through *Whatman* filter paper fungal mass was collected and kept in the oven for overnight drying at 70–80 °C. A control filter paper was also kept in oven simultaneously. The supernatant of the fungal culture was carefully collected and pH change was measured. At the same time initial and final pH of the test compounds (without fungus) were checked and recorded. The pH change of control experiment with ethanol was also checked.

Antioxidant properties

18 mL distilled water was added to 2 mL of Folin Ciocalteu Reagent (FCR) kept in a beaker to make 10 times dilution [28]. 7.5% Na_2CO_3 (7.5 g) solution was prepared in a 100 mL volumetric flask dissolving with distilled water. Stock solution of gallic acid of conc. 1 mg mL^{-1} or 1000 μg mL^{-1} was prepared. Serial dilution was made as required. Blank solution consisting 5 mL Folin-Ciocalteau reagent, 1 mL ethanol and 4 mL sodium carbonate solution (7.5%) was prepared. 2.5 mL of diluted Folin-Ciocalteau reagent, 2.5 mL of sodium carbonate (7.5%) solution was added into the test tube containing 0.5 mL of standard solution. The test tube was incubated for 20 min at 25 °C to complete the reaction. The absorbance of the solution was measured at 760 nm in a spectrophotometer against blank.

The total phenolic content in different concentration levels of standard was calculated in gallic acid equivalents (GAE) by the following formula; C = (c × V)/m. Where, C indicates the total content of phenolic compounds, mg/g standard, in GAE; c indicates the concentration of gallic acid established from the calibration curve, mg/mL; V is the the volume of extract (mL); m is the weight of simple in gram.

Results and discussion

Spectral characterization

*1-(2-hydroxyphenyl)-3-(substituted)furan-prop-2-en-1-one (**1–3**)*

An equimolar mixture of 2-hydroxyacetophenone and furaldehyde in the presence of potassium hydroxide in ethanol was irradiated under microwave condition at 160 W for 3 min 40 sec which afforded 2'-hydroxychalcone derivatives (**1**–**3**) as a crystal (Fig. 1). The compounds are insoluble in H_2O but soluble in organic solvents.

Ź-hydroxychalcone compounds (**1**–**3**) in its IR spectra showed absorption stretching band at 3460–3520 cm^{-1}, 2970–3013.40 cm^{-1}, 1641–1652 cm^{-1}, 1462–1505 cm^{-1}, 1215 cm^{-1} due to presence of –OH, C–H, C=O, C=C (olefinic) and C-O bond, respectively. The spectra also exhibited characteristics of aromatic C=C 1583–1612 cm^{-1} functionality. Absorption stretching band at 1127 cm^{-1} is assigned to -O-CH_3 in

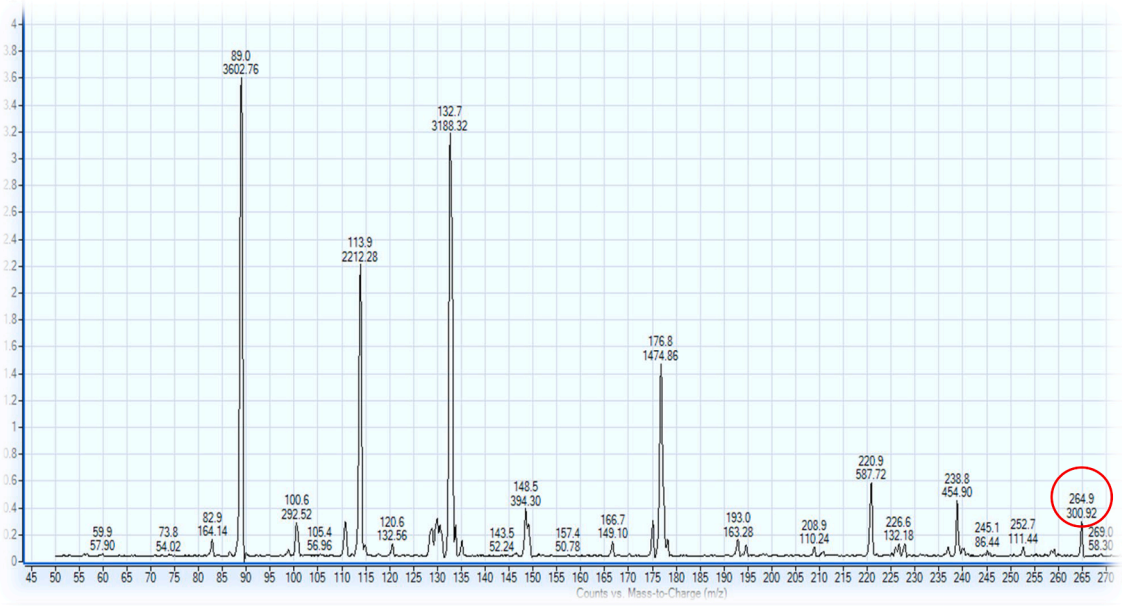

Fig. 3. Mass spectrum of the compound, 2'-hydroxy-4-(N,N-Dimethylamino)chalcone (**6**).

compound **3**.

The ^{1}H NMR spectra of the 2'-hydroxychalcones (**1**–**3**), displayed quartet signal resonated at δ_H 6.57 (J = 7.2 Hz) corresponding to one heteroaromatic proton, C_3-H. One doublet resonated at δ_H 6.80 (J = 8 Hz) corresponding to C_2-H, another doublet signal resonated at δ_H 6.94 due to C_4-H. The compound displayed a doublet signal resonated at δ_H 7.05 (J = 8 Hz) corresponding to one aromatic proton $C_{3'}$-H. This proton coupled with $C_{4'}$-H and produce multiplet signal at δ_H 7.53. The olefinic proton of an α, β unsaturated ketone were clearly observed at δ_H 7.56 (J = 15.2 Hz) and δ_H 7.69 (J = 15.2 Hz) corresponding to C_α-H and C_β-H, respectively. The higher coupling value shows that the two olefinic protons are in *trans*-position. The doublet signal resonated at a lower field, δ_H 7.96 (J = 8 Hz) was attributed to one aromatic proton, $C_{6'}$-H. The ^{1}H NMR spectrum displayed one singlet signal at δ_H 12.90 attributed to presence of one (–OH) group located at $C_{2'}$, respectively. Additional singlet at δ_H 2.61 (3H, s) and 3.78 (3H, s) attributed to $–CH_3$ and $–OCH_3$ in compound **2** and **3**, respectively. Based on these spectral evidences, compounds **(1–3)** were identified as 2'-hydroxychalcone. The *m/z* of molecular peak and elemental analytical data of the compounds (**1**–**3**) are also in good agreement with the assigned structure of the compounds **1**–**3**.

*1-(2'-hydroxyphenyl)-3-(substituted)phenyl-2 propen-1-one **(4–6)***

An equimolar mixture of 2́-hydroxyacetophenone and benzaldehyde or it's derivatives in the presence of potassium hydroxide in ethanol was irradiated under microwave condition at 320 W for 1 min 30 sec afforded desired chalcones (**4**–**6**) as a crystal (Fig. 1).

The compounds **4**–**6** in its IR spectra showed absorption stretching band at 3226 – 3495 cm^{-1}, 2976–3015.12 cm^{-1}, 1670–1692 cm^{-1}, 1575–1636 cm^{-1} and 1230.64 cm^{-1} due to the presence of –OH, C–H,

Table 1
Physicochemical properties, Energy of HOMO-LUMO (eV), hardness, softness and chemical potential and selected vibrational frequencies).

Name	MF	MW		Internal energy	Enthalpy	Free energy	Dipole moment
01	$C_{13}H_{10}O_3$	214.217		−722.812784	−722.811840	−722.866657	4.2348
02	$C_{14}H_{12}O_3$	228.25		−761.894195	−761.893251	−761.952108	4.6949
03	$C_{14}H_{13}O_4$	244.25		−836.676741	−836.675797	−836.737453	3.9138
04	$C_{15}H_{12}O_3$	240.26		−837.654853	− 837.653909	−837.713087	2.5932
05	$C_{15}H_{11}NO_4$	269.26		−928.328034	−928.327090	−928.390989	2.7747
06	$C_{17}H_{17}NO_2$	267.322		−858.149523	−858.148579	−858.216738	7.1328
Name	**HOMO**	**LUMO**		**Gap**	**Hardness**	**Softness**	**Chemical potential**
01	−0.22500	−0.08118		0.14382	0.07191	13.90627	−0.15309
02	−0.22197	−0.07735		0.14462	0.07231	13.82935	−0.14966
03	−0.22647	−0.07340		0.1375	0.076535	13.06592	−0.14994
04	−0.17839	−0.06271		0.11568	0.05784	17.28907	−0.12055
05	−0.23651	−0.1184		0.11804	0.059055	16.93337	−0.17746
06	−0.28771	−0.21124		0.07647	0.038235	26.15405	−0.24948
Compd.	**Assignment**	**Vibrational frequencies (cm^{-1})**		**Compd.**	**Assignment**	**Vibrational frequencies (cm^{-1})**	
		Calculated	**Experimental**			**Calculated**	**Experimental**
01				**06**			
	υO-H	3452	3601		υO-H	3518	3495
	υC-H	3196	3014		υC-H	3013	3015
	υC=O	1640	1641		υC=O	1643	1661
	υC=C	1582	1583		υC=C	1575	1575
	υC=C ph	1487	1474		υC=CPh	1481	1489
	υC-O	1204	1215		υC-N	1324	1339
					υC-O	1206	1230

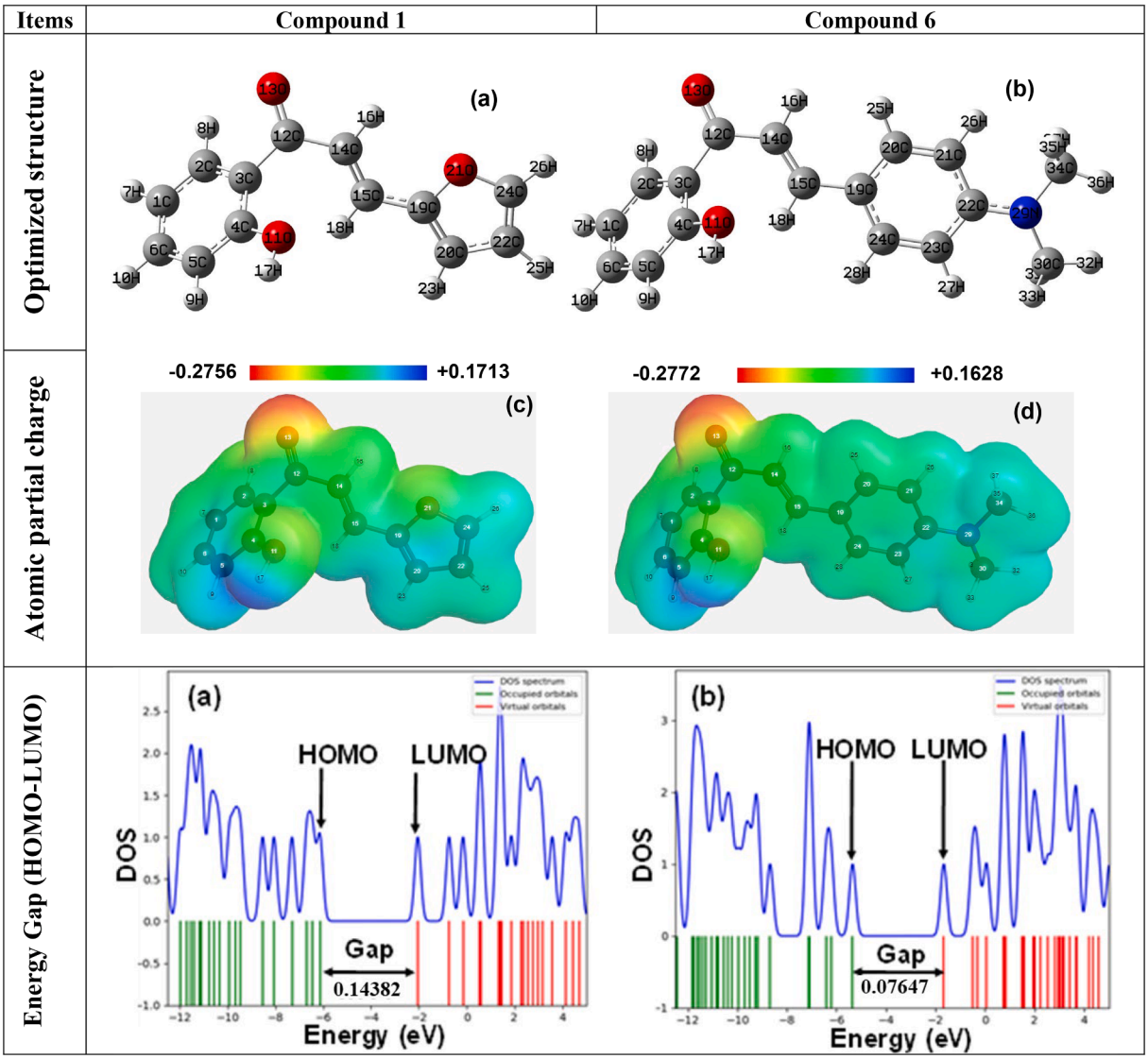

Fig. 4. Optimized structures, atomic partial charges and HOMO-LUMO energy gap of optimized structures.

C=O, C=C (olefinic) and C-O bond, respectively. The spectrum also exhibited characteristics of aromatic C=C functionality 1489–1598 cm^{-1}. Additional peak at 2835 cm^{-1} is due to the presence of $–NO_2$ in compound **5**. Peaks at 1339–1350 cm^{-1} are assigned to C-N in compounds **5** and **6**.

The ^1H NMR spectrum of the compound 2'-hydroxy-4-(N,N-Dimethylamino)chalcone (**6**) as shown in Fig. 2 displayed a one singlet signal resonated at δ_H 3.08 due to presence of two methyl group at C_4 (s, 6H, C_4-N(CH_3)$_2$ attached with electronegative nitrogen atom. One doublet signal resonated at δ_H 7.04 corresponding to one aromatic proton at $C_{3'}$-H. The compound displayed a multiplet signal resonated at δ_H 7.48 corresponding to two aromatic protons, $C_{4'}$-H and $C_{5'}$-H. The presence of two two-proton doublet signals resonated at δ_H 6.74 and δ_H 7.7 with J value 8.0 Hz were designated to C_3-H; C_5-H and C_2-H; C_6-H respectively. The olefinic proton of α, β unsaturated ketone were clearly observed at δ_H 7.61($J = 15.6$ Hz) and δ_H 7.94 ($J = 15.6$ Hz) corresponding to C_α-H and C_β-H, respectively. The higher coupling value shows that the two olefinic protons are in *trans*-position. The doublet signal at a lower field, δ_H 7.96 ($J = 8$ Hz) was attributed to one aromatic proton, $C_{6'}$-H. The ^1H NMR spectrum displayed a singlet signal at δ_H 12.89 attributed to presence of one (–OH) group located at $C_{2'}$, respectively.

Based on these spectral evidences, compounds (**4**–**6**) were identified as 2'-hydroxychalcones. The *m/z* of molecular peak (Fig. 3) and elemental analytical data of the compounds (**4**–**6**) is also in good agreement with the assigned structure. The spectra, however, didn't look explicit probably as isotopic effect.

Computational characterization

Thermodynamic properties and equilibrium geometry

Any modifications in structure significantly influence physicochemical, and binding properties [29]. Internal energy, enthalpy and Gibb's free energy are important thermodynamic factors which regulate the spontaneity of a reaction and stability of a product. Greater negative values are favourable for improved thermodynamic properties. The thermodynamic properties and dipole moment of the compounds are reported in Table 1. The free energy of compounds (**1 – 6)** ranges from −722.866657 to −928.390989 (Hartree), respectively. Improved free energy in compound **5** and dipole moment in compound **6** was observed, which can positively influence the thermodynamic, binding, and interactions properties [30]. Geometry discloses the change of structural properties due to the addition of different functional groups. Bond distances and angles (calculated) depicted in Suppl. Table 1 are approximately same to the theoretical values which support the proposed structures.

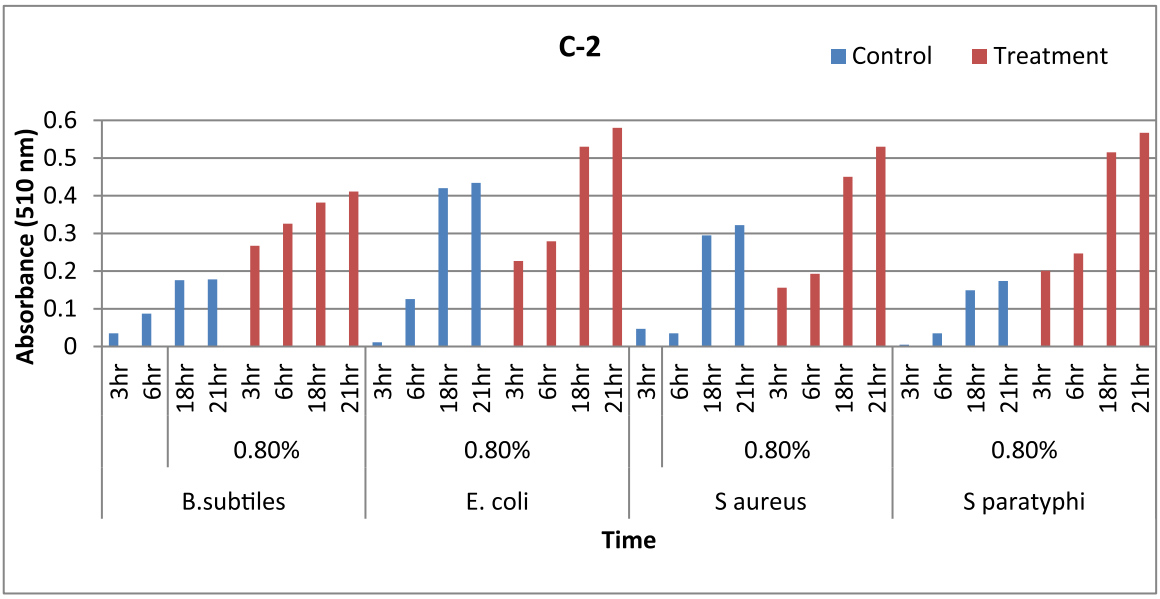

Fig. 5. Antibacterial activity of chalcone-2 at 0.80%.

Molecular electrostatic potential

Electronegative region in molecular electrostatic potential (MEP) which is favorable site for electrophilic attack has been represented by red color. Meanwhile, electropositive site represented by blue colour is the preferred site for nucleophilic attack. Region having the negative potential over oxygen electronegative atoms and that having positive potential over electropositive hydrogen atoms has been focused in MEP. Compound **2** showed the highest electropositive value with high possibility for nucleophilic attack whereas compound **6** showed the highest electronegative value with maximum possibility for electrophilic attack [31].

Molecular orbital analysis

The electronic absorption relates to the transition is electron from the ground to the first excited state. It is described by one electron excitation from the HOMO (highest occupied molecular orbital) to the LUMO (lowest unoccupied molecular orbital). DOS (density of states) plot and HOMO-LUMO energy gap of compound **1** and **6** has been shown in Fig. 4. The HOMO and LUMO energies, energy gap, hardness (η), softness (S) and chemical potential (μ) of all compounds are presented in Table 1. Small HOMO-LUMO energy gap (0.07647 eV) of compound **6** describes its high chemical reactivity and low kinetic stability. Similarly, high kinetic stability and low chemical reactivity associated with large HOMO-LUMO gap (0.14382 eV) of compound **1**. The optimized structures, molecular electrostatic potential graphs and HOMO-LUMO gap values of representative compounds 1 and 6 are shown in Fig. 4. Frontier molecular orbitals (HOMO and LUMO) are displaying in Suppl. Fig. 1.

Vibrational frequency

The stretching vibrations (theoretical IR-frequencies) of the some characteristic bands O–H, C–H, C=O, C-N, C-O, and C–H are compared with those of experimental values of compounds **1** and **6**. Calculated frequencies were scaled by multiplying scaling factor (0.9688) [32]. The experimental and theoretical IR-frequencies of both compounds are tabulated in Table 1. IR spectra obtained by the program are presented in Suppl. Fig. 2. The band observed at 3452 cm^{-1} is due to the OH group in the infrared spectra of the compounds. Presence of stretching vibrations at 3003–3196 cm^{-1} is characteristic to C–H vibrations of the aromatic structure. The bands observed at 1640 and 1582 cm^{-1} are due to υC=O and C=C of the ketoethylenic group. Stretching vibrations observed in the region 1480–1487 cm^{-1} indicated to the presence of aromatic structure C=C. Band observed in the region 1204 cm^{-1} in both compounds is due to C-O bond adjacent to OH substituent. Additional peak in compound **6** due to presence of C-N band was observed in 1324 cm^{-1}. All theoretical IR-frequencies comply with the experimental values.

Biochemical applications

Antimicrobial properties

Effects on selected bacteria

The optical density of *Escherichia coli, Staphylococcus aureus*, *Salmonella paratyphi* and *Bacillus subtilis* were recorded for the test compounds representing the bacterial growth after 3 h to 21 h incubation. Suppl. Figs. 3 and 4 depicts the bacterial growth of tested chalcone (**1**). From the investigation it is seen that chalcone **(1)** showed nearly the same activity as the control against *Bacillus subtilies*, *E. coli, Staphylococcus aureus* and *Salmonella paratyphi*. Maximum growth of bacteria was found at higher concentration against *Salmonella paratyphi* after both 3 h to 21 h incubation. At lower concentration *B. subtilie* and *E. coli* show some inhibiting activity.

Fig. 5 and Suppl. Fig. 5 depict the bacterial growth of test compound**s**. Chalcone (**6**) showed nearly the same activity as the control against *Bacillus subtilies*, *E. coli, Staphylococcus aureus* and *Salmonella paratyphi*. Maximum growth of bacteria was found at higher concentration but in lower concentration growth was minimum of all test organisms. So, the test chalcones (**1, 2, 6**) showed some enhancing capacity after both 3 h to 21 h incubation. In comparison study the antibiotic, ciprofloxacin at lower concentration (0.1%) inhibited the growth of bacteria from 3 h to 21 h incubation in case of *B. Subtilies* and *S. paratyphi*. In case of *E. coli* no induced or inhibition properties was found at lower concentration. The growth of all tested organisms was significantly inhibited with the increase of concentration of samples. It is concluded from the observations that chalcones showed the inducing activity rather than the inhibiting activity against the test organisms.

Effects on selected fungal growth

Fungal growth inhibition of the prepared chalcones was checked against *Aspergillus flavus* and *Aspergillus niger* by the observation fungal growth pattern, pH change and by the determination total biomass. The growth of mycelial mat on the surface of culture supernatant was

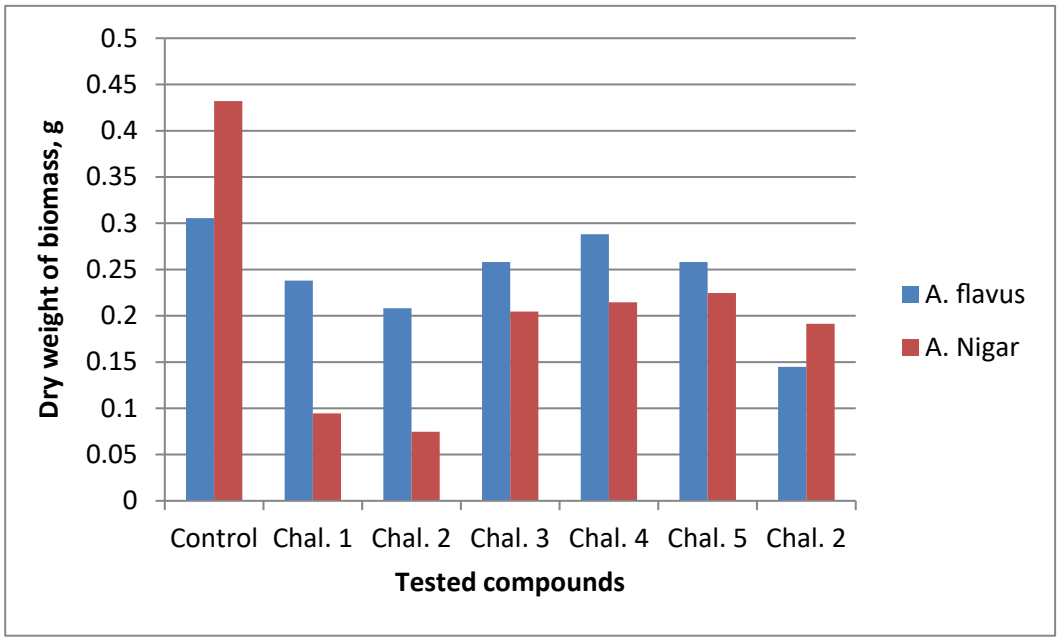

Fig. 6. Dry weight of the total biomass of the treatment and control fungal mycelial mat indicating antifungal role.

observed after optimum incubation periods. The images of sporulation and mat formation captured by digital camera showed that they covered the culture surface in control flask. Whereas, in treatment flask only fungal mat covered the culture surface very small or scanty spore formation observed after the period of 4 days incubation.

The initial and final pH change of the culture broth was recorded. The initial pH of the medium and the final pH level of the positive control were 6.3 and 4.9, respectively. Suppl. Fig. 6 represents the pH of the treatment and control fungal mycelial mat indicating antifungal role. The pH level of 5.3 in treatment flasks was much higher for both tested chalcones against both organisms. The initial and final pH of the cultures in presence of compounds was also recorded. It is found that the changes of pH in presence of compounds were not affecting the final pH of the cultures indicating the inhibition by lower pH values.

The dry weight of the biomass of the treatment and control fungal mycelial mat were determined and compared. The dry weight of the total biomass of the treatment and control fungal mycelial mat has shown in Fig. 6. After the period 4 days incubation the positive control biomass was recorded as 0.31 g for *Aspergillus flavus* and 0.43 g for *Aspergillus niger*. After the same incubation period chalcone **1** and **2** produced 0.26 g and 0.15 g of mycelial mat of *Aspergillus flavus* and 0.10 g and 0.45 g of mycelial mat of *Aspergillus niger,* respectively. Small amount of mat was produced in case of chalcones than the control which indicates the better inhibition property of chalcones against the tested fungi.

Minimum inhibitory concentration (MIC) of the synthesized chalcones was determined by serial broth dilution method. Among the compounds tested, **1, 2, 6** with electron releasing substituents was found

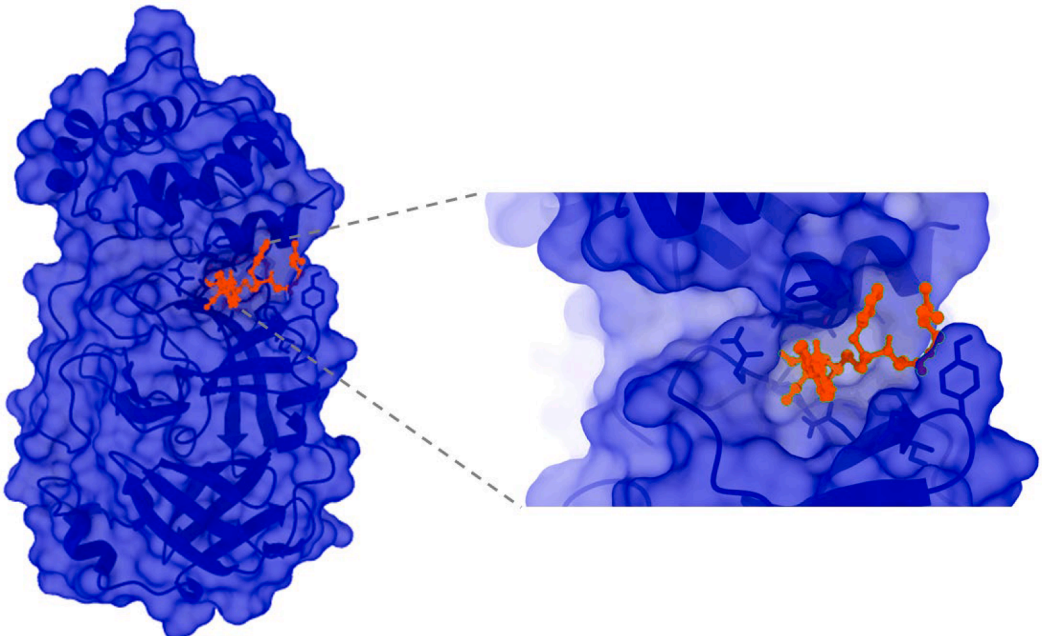

Fig. 7. Docked conformations of **1, 6** and remdesivir and hydroxychloroquine (HCQ) at inhibition binding site of receptor protein (7BQY).

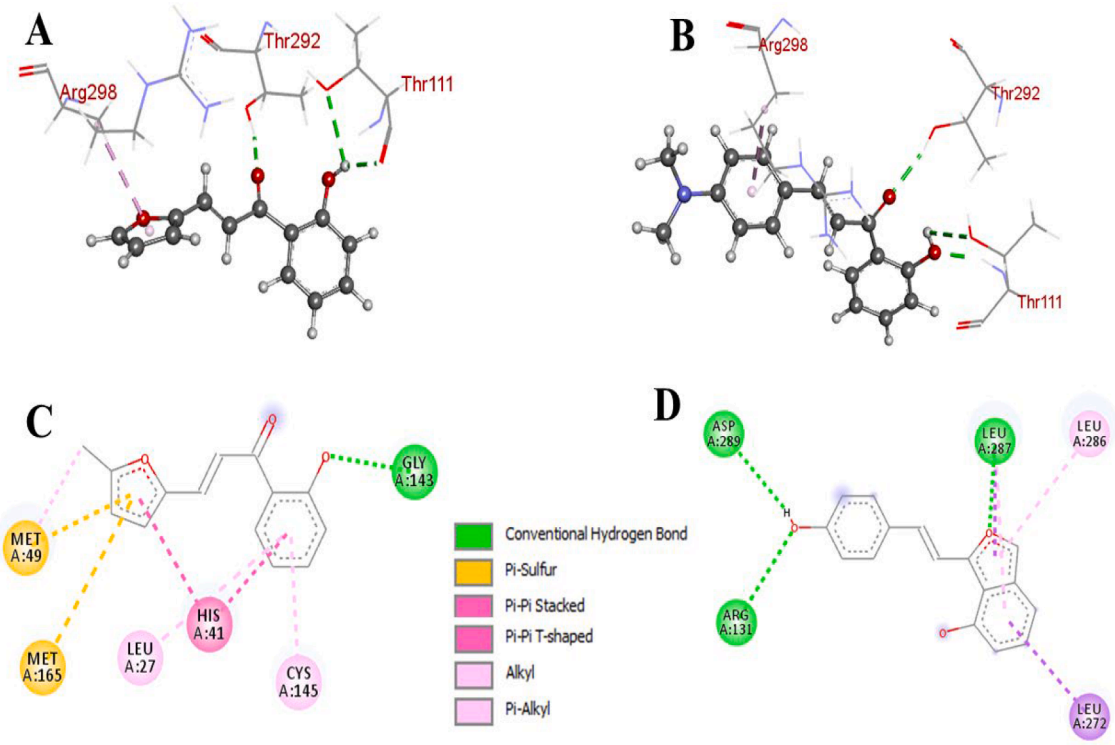

Fig. 8. A & B: Nonbonding (compound **1** and **6)** and C & D: hydrogen bond interactions of chalcones compound (**2 and 4**) with the receptor protein (7BQY), generated by Discovery studio.

Table 2
Binding affinity and nonbonding interaction chalcones.

Compound code	Pyrx (kcal/mol)	Residues in contact, Distance (Å), Interaction type
01	−6.1	THR111 (2.04182) H; THR111 (2.68779) H; THR292 (2.13952) H; ARG298(3.86692)PA
02	−6.4	GLY143 (2.03997) H; MET49 (4.64012) PS; MET165 (5.58544) PS; HIS41 (4.00613) Pi; HIS41 (4.81622) Pi-T; MET49 (3.7371) A; LEU27 (5.3052) PA; CYS145 (4.39946) PA
03	−6.2	GLN110 (2.33019) H; THR111 (1.95153) H; THR292 (2.16072) H; ARG298 (3.85404) PA
04	−6.8	ASP289 (2.7759) H; ARG131 (2.95043) H; LEU287 (1.8963)H; LEU272 (3.8602) Pi-Si; LEU287 (3.89853) Pi-Si; LEU286 (5.03857) PA; LEU287 (5.18171) PA
05	−6.8	THR111 (2.06664) H; THR111 (2.58368) H; THR292 (2.08623) H; ARG298 (3.84075) PA
06	−6.8	THR111 (2.73847) H; THR111 (1.99482) H; THR292 (2.1401) H; ARG298 (3.94618) PA
Remdesivir	−6.7	GLN110 (2.12309) H; THR111 (2.6096) H; THR111 (2.073060H; ASN151 (3.06489) H; ASN151 (2.70568) C; ASP295 (2.12543) C; ILE152 (2.82569) C; ASP153 (2.56878) C; VAL297 (5.45995) A; ARG298 (4.479) A; TYR154 (5.12661) PA; PHE294 (4.68956) PA
HCQ	−5.8	THR111 (2.88215) H; GLN110 (2.49387) C; THR111 (2.99261) C; THR111 (2.19003) C; ARG298 (3.96857) A; ARG298 (4.75658) A; VAL104 (3.84512) A; ILE106 (5.36765) A; PHE294 (5.1869) PA

H: Conventional hydrogen bond, C: Carbon hydrogen bond, A: Alkyl, PA: Pi-alkyl, Pi-T: Pi-Pi T-shaped, PS: Pi-Sulfur, Pi-Si: Pi-Sigma.

to be the most potent having a MIC value of 30 μg mL^{-1} in each case. Other chalcones were also found to be somewhat potent against selective organisms with a MIC of 70 μg mL^{-1}. The structure–activity relationship based on the above results clearly indicated that compounds with electron releasing substituent enhancing the antimicrobial activity.

Molecular docking and nonbonding analysis

In computer aided drug design, molecular docking is a key tool to predict binding affinity, and mode(s) of a ligand with the target [33]. In this study, molecular docking has been performed against SARS-CoV-2 main protease (7BQY) to investigate the binding affinity and inhibiting properties of prepared chalcones considering remdesivir and hydroxychloroquine (HCQ) as standard. The pictorial presentation of molecular docked standard, remdesivir and hydroxychloroquine (HCQ), and chalcones (**1, 6**) against receptor protein 7BQY is as in Fig. 7.

Fig. 8 shows nonbonding interactions of chalcones **1 & 6** with the receptor protein (7BQY) generated by Discovery studio. Binding affinity and nonbonding interaction of standard, remdesivir and hydroxychloroquine (HCQ) and prepared chalcones after rigid docking with receptor protein 7BQY are given in Table 2. The binding affinity of remdesivir and hydroxychloroquine (HCQ) is −6.7 and −5.8 kcal/mol, respectively whereas that of chalcones **4**–**6** has considerably increased to −6.8 kcal/mol. The highest binding affinity may contribute significant hydrogen bond (HB) formation with the amino acid residues of target protein [33]. From docking results, it confirms the simultaneous binding ability of chalcones to the active site of protein. It further supports them as potential candidate for the inhibiting of SARS-CoV-2 protease. Standards, Remdesivir and hydroxychloroquine (HCQ), and chalcone derivatives were bound at the same binding pocket of receptor protein and superimposed to each other. Important conventional hydrogen bond, and carbon hydrogen bonds were observed in all compounds. HB with < 2.3 Å significantly influence the binding affinity and specialty in different magnitude [34]. Some common significant HBs were observed in both compounds with the amino acid residues (Thr111, Thr292) of receptor protein (7BQY) and they were relatively smaller than remdesivir. Thr111, Thr292, Arg298, Tyr154, and Gln110 residues commonly play key to improve the interactions. Pi-alkyl (PA) bond interactions with Leu286, Leu287, Cys145, Arg298, Tyr154, Phe294 are possibly

Table 3
Selected pharmacokinetic characteristics of chalcones.

Pharmacokinetic parameters						
Drug	Blood brain barrier	Human intestinal absorption	P-glyco protein inhibitor	hERG	Carcinogen	Rat acute toxicity LD_{50} (mol/Kg)
01	+(0.9649)	+(1.0000)	NI(0.9552)	WI(0.9054)	NC(0.8952)	2.2218
02	+(0.8627)	+0.9766	−0.853	WI(0.6531)	NC(0.7316)	3.198e
03	+(0.9405)	+0.9685	−0.7184	WI(0.5202)	NC(0.8055)	2.8937
04	−0.756	+0.9803	−0.9628	WI(0.8706)	NC(0.5367)	2.9935
05	+(0.8939)	+0.9155	−0.9675	WI(0.8812)	NC(0.5032)	3.2342
06	+(0.8543)	+(0.9967)	NI(0.8171)	WI(0.8959)	NC(0.6455)	2.3208

NI: Non-inhibitor, WI: Weak inhibitor, NC: Non-carcinogen.

considered for the higher affinity of tested chalcones than remdesivir and His41 showed Pi and Pi-Pi-T shaped interactions showed in compound 2.

ADMET analysis

From ADMET results, it is found that all the molecules have positive response for blood brain barrier and human intestinal absorption. Which predicting that they can pass through the BBB and absorbed by intestine. They are non-carcinogenic and have no inhibition to P-glycoprotein, where inhibition can block the absorption, permeability and retention of the chemicals [35]. Selected pharmacokinetics parameters are reported in Table 3**.** However, all compounds showed weak inhibitory property for human ether-a-go-go-related gene (hERG). As hERG inhibition leads to long QT syndrome more study of this phase is required.

Antioxidant properties, total phenolic content

The compounds having good antioxidant properties are supposed to possess biological properties like anti-apoptosis, anti-aging, anti-carcinogen, anti-inflammation, anti-atherosclerosis, cardiovascular protection and improvement of endothelial function. Inhibition of angiogenesis and cell proliferation activities are also for such compounds. It might have the anti-inflammation, anti-atherosclerosis and the antioxidant properties. Investigation showed the total phenolic content (TPC) of prepared chalcones (**1**–**6)** 212.27 ± 1.48, 225.64 ± 3.17, 213.05 ± 2.04, 145.34 ± 2.13, 239.61 ± 3.17 and 164.22 ± 2.56 mg g^{-1}, respectively. These results indicate that they have good antioxidant properties which are attributable to phenolic –OH group attached to the ring structures. Pyrazolic chalcones are reported to possess higher antioxidant ability.

Conclusion

In this study six new 2́-hydroxychalcone derivatives were synthesized by microwave assisted method and characterized by spectral (FT-IR, UV–Vis, ^{1}H NMR, and MS), physicochemical analysis. Antimicrobial, antioxidant, molecular docking, nonbonding interactions, and pharmacokinetic studies were performed to evaluate the biological/biomedical, and biochemical performance. Compounds showed good inhibition against tested pathogenic organisms and possessed good antioxidant properties. ADMET prediction disclosed that synthesized chalcones are non-carcinogenic and relatively less toxic. Molecular docking study suggested their improved inhibition to the SARS-CoV-2 main protease than remdesivir compare to hydroxychloroquine (HCQ).

Funding

This research was conducted by partial financial grant from Publication and Research Cell, University of Chittagong, Bangladesh.

CRediT authorship contribution statement

Mohammad Nasir Uddin: Conceptualization, Writing – review & editing. **Sayeda Samina Ahmed:** . **Monir Uzzaman:** . **Md. Nazmul Hassan Knock:** Formal analysis. **Wahhida Shumi:** . **Abul Fazal Md. Sanaullah:** Writing – review & editing. **Md. Mosharef Hossain Bhuyain:** .

Declaration of Competing Interest

The authors declare that they have no known competing financial interests or personal relationships that could have appeared to influence the work reported in this paper.

Acknowledgements

The authors wish to acknowledge to Department of Chemistry and Department of Microbiology for infrastructural support and to Publication and Research Cell, University of Chittagong, Bangladesh for partial financial support to conduct the research.

Appendix A. Supplementary data

Supplementary data to this article can be found online at https://doi.org/10.1016/j.rechem.2022.100329.

References

[1] T. Acter, N. Uddin, J. Das, A. Akhter, T.R. Choudhury, S. Kim, Evolution of Severe Acute Respiratory Syndrome Coronavirus 2 (SARS-CoV-2) as Coronavirus Disease 2019 (COVID-19) Pandemic: A Global Health Emergency, Sci. Total Environ. (2020) 138996.
[2] D.L. Barnard, D.F. Smee, J.H. Huffman, L.R. Meyerson, R.W. Sidwell, Antiherpesvirus Activity and Mode of Action of SP-303, a Novel Plant Flavonoid, Chemotherapy 39 (1993) 203–211.
[3] N. De Meyer, A. Haemers, L. Mishra, H.K. Pandey, L.A. Pieters, D.A. Vanden Berghe, A.J. Vlietinck, 4'-Hydroxy-3-methoxyflavones With Potent Antipicornavirus Activity, J. Med. Chem. 34 (1991) 736–746.
[4] S.K. Awasthi, N. Mishra, B. Kumar, M. Sharma, A. Bhattacharya, L.C. Mishra, V. K. Bhasin, Potent antimalarial activity of newly synthesized substituted chalcone analogs in vitro, Med. Chem. Res. 18 (6) (2009) 407–420.
[5] S.S. Lim, H.S. Kim, D.U. Lee, In-vitro antimalarial activity of flavonoids and chalcones, Bull. Korean Chem. Soc. 28 (2007) 2495–2497.
[6] T.S. Straub, Epoxidation of α, β-unsaturated ketones with sodium perborate, Tetrahedron Lett. 36 (1995) 663–664.
[7] T. Tran, H. Park, H.P. Kim, G.F. Ecker, K. Thai, Inhibitory activity of prostaglandin E2 production by the synthetic 2́-hydroxychalcone analogues: Synthesis and SAR study, Bioorg. Med. Chem. Lett. 19 (2009) 1650–1655.
[8] D.K. Mahapatra, S.K. Bharti, V. Asati, Chalcone scaffolds as anti-infective agents: structural and molecular target perspectives, Eur. J. Med. Chem. 101 (2015) 496–524.
[9] S. Jo, H. Kim, S. Kim, D.H. Shin, M.-S. Kim, Characteristics of flavonoids as potent MERS-CoV 3C-like protease inhibitors, Chem. Biol. Drug Des. 94 (6) (2019) 2023–2030.
[10] T.T. Dao, P.H. Nguyen, H.S. Lee, E. Kim, J. Park, S.I. Lim, W.K. Oh, Chalcones as novel influenza A (H1N1) neuraminidase inhibitors from Glycyrrhiza inflata, Bioorg. Med. Chem. Lett. 21 (1) (2011) 294–298.
[11] C.-W. Lin, F.-J. Tsai, C.-H. Tsai, C.-C. Lai, L. Wan, T.-Y. Ho, C.-C. Hsieh, P.-D. Chao, Anti-SARS coronavirus 3Clike protease effects of Isatis indigotica root and plant derived phenolic compounds, Antiviral Res. 68 (1) (2005) 36–42.

[12] V. Patil, S.A. Patil, R. Patil, A. Bugarin, K. Beaman, S.A. Patil, Exploration of (hetero)aryl derived thienylchalcones for antiviral and anticancer activities, Med. Chem. 15 (2) (2019) 150–161.
[13] J.-Y. Park, J.-A. Ko, D.W. Kim, Y.M. Kim, H.-J. Kwon, H.J. Jeong, C.Y. Kim, K. H. Park, W.S. Lee, Y.B. Ryu, Chalcones isolated from Angelica keiskei inhibit cysteine proteases of SARS-CoV, J. Enzyme Inhib. Med. Chem. 31 (1) (2016) 23–30.
[14] M.P. Gleeson, D. Gleeson, QM/MM Calculations in Drug Discovery: A Useful Method for Studying Binding Phenomena? J. Chem. Inf. Model. 49 (2009) 670.
[15] M.J. Frisch, G.W. Trucks, H.B. Schlegel, G.E. Scuseria, M.A. Robb, J.R. Cheeseman, G. Scalmani, V. Barone, G.A. Petersson, H. Nakatsuji, Gaussian 16. Revis. A 3 (2016).
[16] A.D. Becke, Density-functional exchange-energy approximation with correct asymptotic behavior, Phys. Rev. A 38 (6) (1988) 3098–3100.
[17] C. Lee, W. Yang, R.G. Parr, Development of the Colle-Salvetti correlation-energy formula into a functional of the electron density, Phys. Rev. B 37 (1988) 785.
[18] H.P. Ebrahimi, J.S. Hadi, Z.A. Abdulnabi, Z. Bolandnazar, Spectroscopic, thermal analysis and DFT computational studies of salen-type Schiff base complexes, Spectrochim. Acta Part A Mol. Biomol. Spectrosc. 117 (2014) 485.
[19] R.G. Pearson, The HSAB Principle — more quantitative aspects, Inorg. Chim. Acta 240 (1995) 93–98.
[20] F. Azam, N.H. Alabdullah, H.M. Ehmedat, A.R. Abulifa, I. Taban, S. Upadhyayula, NSAIDs as potential treatment option for preventing amyloid β toxicity in Alzheimer's disease: an investigation by docking, molecular dynamics, and DFT studies, J. Biomol. Struct. Dyn. 36 (2018) 2099–2117.
[21] M.J. Lucido, B.J. Orlando, A.J. Vecchio, M.G. Malkowski, Crystal structure of aspirin-acetylated human cyclooxygenase-2: Insight in to the formation of products with reversed Stereochemistry, Biochemistry 55 (2016) 1226.
[22] N. Guex, M.C. Peitsch, SWISS-MODEL and the Swiss-PdbViewer: An Environment for Comparative Protein Modeling, Electrophoresis 18 (1997) 2714–2723.
[23] W.L. Delano, The PyMOL Molecular Graphics System. De-Lano Scientific, San Carlos, CA, USA. Http://www.pymol.org. (2002).
[24] S. Dallakyan, A.J. Olson, Small-Molecule Library Screening by Docking with PyRx, in: J.E. Hempel, C.H. Williams, C.C. Hong (Eds.), Chem, Biol. Methods Protoc, Springer, New York, New York, NY, 2015, p. 243.
[25] F. Cheng, W. Li, Y. Zhou, J. Shen, Z. Wu, G. Liu, P.W. Lee, Y. Tang, AdmetSAR: A Comprehensive Source and Free Tool for Assessment of Chemical ADMET Properties, J. Chem. Inf. Model. 52 (2012) 3099–3105.
[26] M.N. Uddin, S. Khandaker, M. Uzzaman, M.S. Amin, W. Shumi, M.A. Rahman, S. M. Rahman, Synthesis, characterization, molecular modeling, antioxidant and microbial properties of some Titanium(IV) complexes of Schiff bases, J. Mol. Struct. 1166 (2018) 79.
[27] M.N. Uddin, D.A. Chowdhury, N. Mase, M.F. Rashid, M. Uzzaman, A. Ahsan, N. M. Shah, Spectral and computational chemistry studies for the optimization of geometry of dioxomolybdenum(VI) complexes of some unsymmetrical Schiff bases as antimicrobial agent, J. Coord. Chem. 71 (23) (2018) 3874–3892.
[28] M.N. Uddin, Z.A. Siddique, N. Mase, M. Uzzaman, W. Shumi, Oxotitanium(IV) complexes of some bis-unsymmetric Schiff bases: Synthesis, structural elucidation and biomedical applications, Appl. Organometal. Chem. (2019) e4876.
[29] M. Uzzaman, T. Mahmud, Structural Modification of Aspirin to Design a New Potential Cyclooxygenase (COX-2) Inhibitors, Silico Pharmacol. 8 (1) (2020) 1–14.
[30] M. Uzzaman, M.N. Uddin, Optimization of Structures, Biochemical Properties of Ketorolac and Its Degradation Products Based on Computational Studies. DARU, J. Pharm. Sci. 27 (1) (2019) 71–82.
[31] M. Uzzaman, J. Shawon, Z.A. Siddique, Molecular Docking, Dynamics Simulation and ADMET Prediction of Acetaminophen and Its Modified Derivatives Based on Quantum Calculations, SN Appl. Sci. 1 (11) (2019) 1437.
[32] A.V. Marenich, C.J. Cramer, D.G. Truhlar, Universal Solvation Model Based on Solute Electron Density and on a Continuum Model of the Solvent Defined by the Bulk Dielectric Constant and Atomic Surface Tensions, J. Phys. Chem. B 113 (18) (2009) 6378–6396.
[33] G.M. Morris, M. Lim-Wilby, Molecular Docking BT - Molecular Modeling of Proteins, in: Kukol (Ed.), Humana Press, Totowa, NJ, 2008, pp. 365.
[34] V.B. Zhurkin, M.Y. Tolstorukov, F. Xu, A.V. Colasanti, W.K. Olson, The Role of Hydrogen-Bonds in Drug Binding, in: DNA Conformation and Transcription; Springer US: Boston, MA, 2005, pp 18–34.
[35] M.L. Amin, P-glycoprotein Inhibition for Optimal Drug Delivery, Drug Target Insights 7 (2013) 27–34.